

Unexpected behavior of the antiferromagnetic mode of NiO

M. Grimsditch

Materials Science Division, Argonne National Laboratory, Argonne, Illinois 60439

L. E. McNeil

Department of Physics and Astronomy, University of North Carolina at Chapel Hill, Chapel Hill, North Carolina 27599-3255

D. J. Lockwood

Institute for Microstructural Sciences, National Research Council of Canada, Ottawa, Ontario, Canada, K1A 0R6

(Received 19 December 1997)

Although NiO is often considered the classic example of an antiferromagnetic insulator, recent investigations have revealed unexplained features of the magnon spectrum. The present study of the temperature and polarization behavior of first-order magnetic Raman scattering reveals that the polarization selection rules are not described by the generally accepted antisymmetric scattering tensor. The inclusion of quadratic magneto-optic coupling terms can explain the symmetry of the scattering tensor, but does not lead to results consistent with the accepted [112] spin alignment direction. [S0163-1829(98)06241-9]

INTRODUCTION

NiO is frequently cited as the exemplar of an antiferromagnetic (AF) insulator. Its simple NaCl crystal structure and type-II fcc spin pattern have made it an attractive choice for qualitative and quantitative theoretical studies of its magnetic properties, as well as for experimental investigations using neutron and light scattering.¹⁻⁹

Given this long tradition of attention to NiO and the simplicity of its most obvious features, one might think that there is little further to be learned by examining it once more. However, three recent articles⁷⁻⁹ showed that, contrary to expectation, the first-order Raman AF magnon appears as a doublet rather than a singlet. Also, the Brillouin spectrum⁹ of NiO contains a broad central feature that, although not yet identified, is certainly of magnetic origin since it vanishes at the Néel temperature ($T_N = 523$ K). We have therefore reinvestigated NiO by performing a light-scattering study of the polarization and temperature dependence of the single-magnon excitation. The temperature dependence of the magnon frequency is consistent with previous experimental⁷ and theoretical¹⁰ studies, but its polarization features are inconsistent with the common assumption that magnetic scattering is dominated by antisymmetric scattering.

An analysis of the theory of magnetic scattering in NiO explains why the antisymmetric scattering is weak and therefore why it is dominated by the, usually smaller, quadratic coupling terms that lead to symmetric scattering tensors. Although the inclusion of quadratic coupling explains the symmetric nature of the observed scattering, the resulting predictions for polarization features of the magnon are not consistent with the accepted [112] spin orientation. Possible origins of this discrepancy are discussed; we believe that the most likely explanation is that the spins are aligned along $\langle 100 \rangle$ directions.

EXPERIMENT

In these experiments we used a green-colored NiO sample grown by chemical vapor deposition on the (100) face of a

MgO crystal. This sample is identical to that used in a previous study in our laboratory⁹ except that we did not remove the substrate. Details of the sample preparation and characterization can be found in Ref. 9.

We varied the temperature over the range 9–300 K by affixing the sample with GE varnish to the cold finger of a variable temperature cryostat. For measurements above room temperature we varnished the sample to a resistance heating element and heated it in air up to 475 K, which is 0.91 of the Néel temperature.

To excite the magnon spectra we used the 476.2-nm and 647.1-nm lines of a Kr⁺ laser, with output powers in the range 40–200 mW. The polarization of the incident beam was controlled by a polarizing prism, followed by a polarization rotator or a Babinet compensator. (We note that the polarizing prism guarantees that the laser plasma lines have the same polarization as the laser radiation.) We observed the spectra with a charge-coupled device (CCD) detector system attached to a triple spectrometer. Where necessary, a Ne lamp, positioned so that its emission lines were introduced into the spectrum, provided us with a fiducial to correct for possible drifts in the CCD or spectrometer positions.

TEMPERATURE STUDY

Typical spectra at low and room temperatures are shown in Fig. 1. Previous studies⁷⁻⁹ found that the magnon develops a doublet structure as the temperature is lowered. In this investigation the doublet structure is never clearly resolved even at the lowest temperatures achieved: we believe this may be due to small residual strains induced because the NiO was not removed from the MgO substrate. In spite of not being able to resolve the two peaks, the frequency of the shoulder, seen in the 35-K spectrum in Fig. 1, can be obtained from a curve fitting routine.

The circles in Fig. 2 represent our measurements of the temperature dependence of the frequency of the one-magnon peak. Below approximately 260 K ($T/T_N \sim 0.5$) the peak in

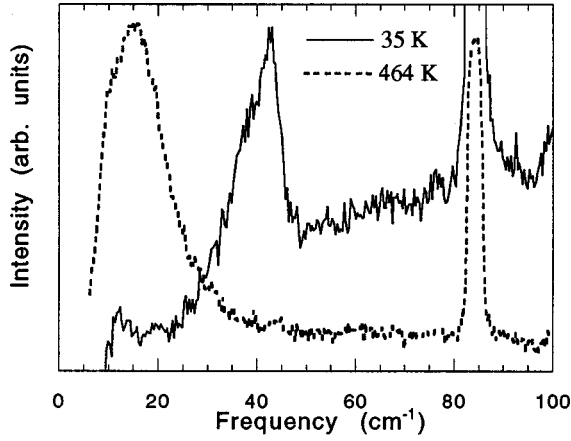


FIG. 1. Magnon spectra of NiO, obtained with 647.1-nm radiation, at low and high temperatures. No analyzer was used in the collection beam. Solid line: 35 K; dashed line: 464 K. The peak at 84 cm^{-1} is an emission line from a Ne lamp, used as a fiducial. The instrument resolution (3.5 cm^{-1}) is given by the width of the Ne emission line at 84 cm^{-1} .

the light scattering spectrum develops a structure that can be fit by a doublet; open and full symbols represent the high and low frequency components, respectively. Below approximately 210 K ($T/T_N \sim 0.4$) the frequencies of the two peaks remain constant with temperature, and are separated by $\sim 5 \text{ cm}^{-1}$. The results shown in Fig. 2 are in excellent agreement with those in Ref. 7, which were obtained on a black (oxygen deficient) NiO crystal, and with that in Ref. 9 obtained from the same sample used here but removed from the substrate.

The solid line in Fig. 2 is the theoretical prediction (Fig. 3 of Cottam and Awang¹⁰) for the $\mathbf{k}=0$ magnon frequency in NiO as a function of temperature.¹¹ The values used in Ref. 10 for the exchange and single-ion anisotropy parameters were obtained from the neutron scattering experiments of Hutchings and Samuelsen.⁵ The close agreement between the measured and calculated temperature dependence confirms that the peak we observe in our light-scattering spectra is indeed the single-magnon AF excitation, and that existing theories account well for the behavior of its frequency as a function of temperature.

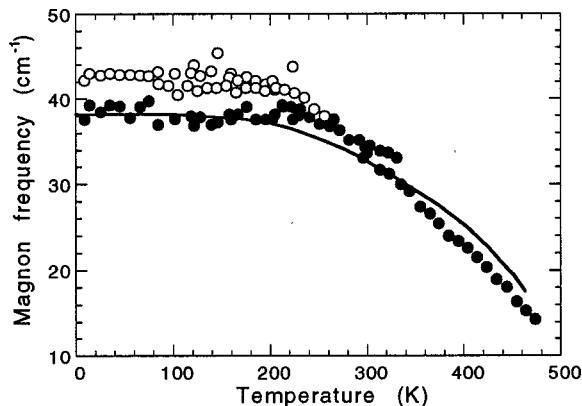


FIG. 2. Temperature dependence of the NiO magnon frequency. Symbols are our experimental results, the full line is the calculation from Ref. 10.

It is worth noting that there is no generally accepted definition of the anisotropy parameters in NiO, Stevens¹² and Cottam and Awang¹⁰ define the anisotropies in terms of spin values squared but use slightly different Hamiltonians. Cottam and Lockwood¹³ define the anisotropy to be linear in spin. All the formulations, however, lead to expressions for the magnon frequencies that have equivalent functional forms and hence imply that the different definitions are probably equivalent. Great care must therefore be taken when using numerical values for the anisotropies to ensure that they correspond to the formulation in which they are being used. The problem is further complicated since the (appropriately transformed) anisotropy parameters extracted from the same neutron data⁵ are slightly different in Refs. 10 and 12. Fortunately this has only a small effect on the frequency of the magnon mode observed with Raman scattering (Figs. 1 and 2), but it has a pronounced effect on the frequency of an even lower mode that has never been experimentally observed. We shall return to this point in the Discussion section.

POLARIZATION STUDY

In Fig. 3 we show spectra recorded in the near-backscattering geometry with the propagation vectors, k_i and k_s , close to the [001] direction. The incident and scattered polarizations are indicated in each spectrum. The surprising feature exhibited by these spectra is that they are *not* consistent with the usually accepted predictions, based on linear magneto-optic coupling, that magnetic scattering is described by an antisymmetric tensor.^{3-10,12,14} In general, though, the inclusion of quadratic coupling results in a asymmetric scattering tensors.

To confirm that we have correctly identified the polarization in each spectrum we note that the intensity of the plasma line from the laser near 14 cm^{-1} is a clear indication that our polarizations are indeed as specified and that our intensity selection rules are not due to mislabeling—the plasma line is strong for incident and scattered polarizations parallel to one another but weak otherwise. We mention also that the selection rules were verified both by rotating the polarization of the incident light and by rotating the sample. Furthermore, experiments were performed both in backscattering and in near-forward scattering and with 476- and 647-nm radiation. All our results confirmed the polarization features shown in Fig. 3 and collected in Table I.

We first show that the polarization features in Fig. 3 are inconsistent with an antisymmetric scattering tensor. We will return below to the more general aspects of scattering cross sections and the considerations that lead to symmetric or antisymmetric scattering tensors. The most general antisymmetric tensor T_{AS} is

$$\begin{pmatrix} 0 & a & b \\ -a & 0 & c \\ -b & -c & 0 \end{pmatrix}.$$

Intensities expected from such a tensor are $|e_i T_{AS} e_s|^2$, where e_i and e_s are the incident and scattered light polarizations. For the case of incident and scattered light propagating along the [001] direction, the expected intensities for various

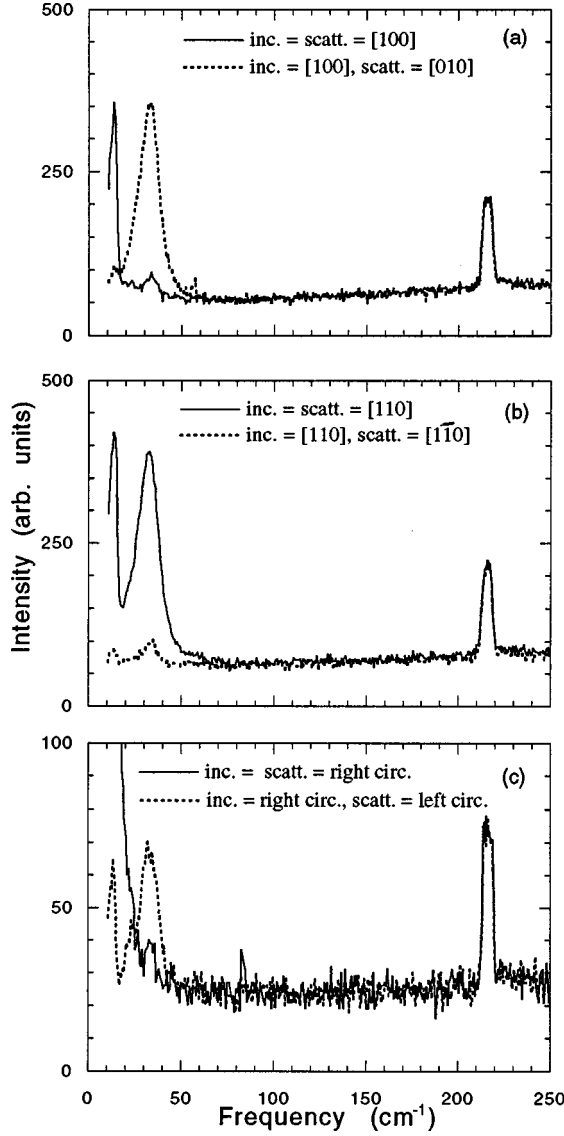


FIG. 3. Polarization features of the first-order magnon line of NiO at room temperature. All spectra were recorded in quasibackscattering from a (001) surface using 476.2-nm radiation. The peak at 215 cm^{-1} is an emission line from a Ne lamp, used as a fiducial. (a) Solid line: incident and scattered polarization along [100]. Dashed line: incident polarization along [100], scattered polarization along [010]. (b) Solid line: incident and scattered polarization along [110]. Dashed line: incident polarization along [110], scattered polarization along [110]. (c) Solid line: incident and scattered polarization right circular. Dashed line: incident polarization right circular, scattered polarization left circular.

incident and scattered polarizations are listed (I_{AS}) in Table I. Note that for antisymmetric scattering the scattered light never has the same polarization as the incident polarization, a fact contradicted by the experimental results with [110] polarization shown in Fig. 3. Furthermore, since the antisymmetric nature of the scattering tensor is unaffected by crystal orientation, including the possibility of multiple domains in our sample cannot account for the results in Fig. 3.

We now return to the issue of why an antisymmetric scattering tensor is often assumed for magnetic scattering. We will follow the notation used in Ref. 13, which has conveniently consolidated the original contributions in this field.

We consider first only linear magneto-optic coupling, which leads to antisymmetric scattering. The phenomenological relations used in magneto-optics are [Eq. (2.64) of Ref. 13]

$$\Delta X^{\alpha\beta} = K_{\alpha\beta\mu} S^{\mu}, \quad (1)$$

where ΔX is the polarizability change induced by a spin S . In a cubic material like NiO the complex tensor \mathbf{K} can be shown to possess zeros if two indices are repeated and there is only one independent element $K = K_{xyz} = K_{zxy} = K_{yzx} = -K_{zyx} = -K_{xzy} = -K_{yxz}$. It is these latter relations that determine that the resulting scattering tensor is antisymmetric. The Hamiltonian for one-magnon light scattering is then shown to consist of four terms [Eq. (5.9), Ref. 13]: $(K_1 + K_2)\{S_{1-} + S_{2-}\}$, $(K_1 + K_2)\{S_{1+} + S_{2+}\}$, $(K_1 + K_2)\{S_{1-} - S_{2-}\}$, and $(K_1 - K_2)\{S_{1+} - S_{2+}\}$ where 1 and 2 represent the two AF sublattices and S^- and S^+ are spin operators corresponding to Stokes (magnon creation) and anti-Stokes (magnon annihilation) Raman scattering. In the case of NiO, where the two sublattices are related by a translation, symmetry requires that $K_1 = K_2$ so that only the first two terms above remain. In the nomenclature of Ref. 13 only ‘‘in phase’’ scattering [Eq. (5.9), Ref. 13] is allowed by symmetry.

The remaining step is to estimate the spin-dependent terms appearing in the Raman intensity expressions. The expression that describes the integrated intensity (I) for in-phase one magnon Stokes scattering is [Eq. (5.17), Ref. 13]

$$I \propto \langle S^Z \rangle [\omega_A / \omega_A + 2\omega_E]^{1/2} |K_+|^2 \times |e_i^z e_S^+ - e_i^+ e_S^z|^2 [n(\omega) + 1], \quad (2)$$

where $K_+ = (K_1 + K_2)/2$, the anisotropy frequency $\omega_A (= g \mu_B D)$, where g is the ‘‘ g ’’ factor, μ_B the Bohr magneton, and D the effective anisotropy field) and the exchange frequency $\omega_E (= \langle S^Z \rangle J)$, where z defines the spin alignment direction and J is the exchange). e_i and e_S are polarization indices for the incident and scattered light, the superscript + denotes right circular polarization ($x + iy$), and $[n(\omega) + 1]$ is the thermal population factor. Thus at low temperature ($\ll T_N$) the Raman intensity depends on the spin expectation value $\langle S^Z \rangle \approx S = 1$, the anisotropy and exchange terms, and the linear magneto-optic coupling coefficient K_+ . For NiO, $\omega_E = 918 \text{ cm}^{-1}$ (this is $6J_2$ in the nomenclature of Ref. 12) and $\omega_A < 0.8 \text{ cm}^{-1}$ (the value depending slightly on the choice of following the nomenclature of Ref. 10 or 12) so that $R = [\omega_A / (\omega_A + 2\omega_E)]^{1/2} < 0.02$. The weak, or absence of, antisymmetric scattering in Ni can therefore be traced to the small value for the prefactor in Eq. (2). Although this conclusion is consistent with the observation¹⁵ of antisymmetric scattering in tetragonal FeF_2 where the prefactor is $R = 0.38$,¹⁵ it is noteworthy that antisymmetric scattering is also observed in isomorphous MnF_2 where $R = 0.09$.¹⁶ We shall return to this issue in the next section.

We turn now to the scattering in NiO including the contribution of quadratic magneto-optic coupling (G_1 and G_2) as originally developed by Cottam.¹⁴ Experimentally the quadratic terms were found to be significant in FeF_2 ¹⁵ and MnF_2 .^{16,17} In the absence of linear coupling the integrated Raman intensity of in-phase Stokes scattering is given by [Eqs. (5.19) and (5.21), Ref. 13]

TABLE I. Measured polarization features of the first-order Raman magnon mode of NiO and selection rules predicted for an antisymmetric scattering tensor, and for symmetric tensors originating from specific spin orientations. e_i and e_s are the directions of the incident and scattered light polarizations, I_{expt} is the experimentally observed intensity, I_{AS} is the intensity calculated for an antisymmetric tensor, $[jkl]$ is intensity calculated for a symmetric scattering tensor originating from a spin along the $[jkl]$ direction.

e_i	e_s	I_{expt}	I_{AS}	[100]	[010]	[001]	[110]	[101]	[011]	[112]
[100]	[100]	weak	0	0	0	0	1	1	0	1.0
[100]	[010]	strong	1	1	1	0	0	0.5	0.5	0.22
[110]	[110]	strong	0	1	1	0	0	1.46	1.46	0.89
[110]	[$\bar{1}\bar{1}$ 0]	weak	1	0	0	0	1	0.25	0.25	0.33
[1 <i>i</i> 0]	[1 <i>i</i> 0]	weak	0	0	0	0	0	0.25	0.25	0.22
[1 <i>i</i> 0]	[1- <i>i</i> 0]	strong	1	1	1	0	1	0.75	0.75	0.56

$$I \propto (\langle S^Z \rangle)^3 p^2 [\omega_A / (\omega_A + 2\omega_E)]^{-1/2} |G_+|^2 \times |e_i^z e_s + e_i^+ e_s^-|^2 [n(\omega) + 1], \quad (3)$$

where $G_+ = (G_1 + G_2)/2$ and p is a numerical factor close to 1 for NiO at low temperatures. Compared to Eq. (2), important to note are the plus sign in the polarization term, which leads to symmetric scattering, and the change in sign in the power of the prefactor, which makes it >50 for NiO instead of <0.02 . In a reference frame in which the x axis is along the spin direction, the scattering tensor predicted by Eq. (3) takes on the form^{12,14}

$$\begin{pmatrix} 0 & a & a \\ a & 0 & 0 \\ a & 0 & 0 \end{pmatrix}.$$

On rotating this tensor into the crystallographic reference frame it retains its symmetric character but, for an arbitrary spin direction, all its elements will be nonzero and would lead to scattered light with no clear polarization features.

Interpretation of experimental data is complicated by the domain structure that exists in most NiO samples. The reproducibility of our observed polarization selection rules obtained in different scattering geometries is consistent with either a single domain sample or a sample in which the domains are much smaller than the 100- μm laser spot. Because we have no way of experimentally evaluating the domain structure, we deal with the domain aspect in the calculations instead. To include this effect we have listed in Table I the predicted intensities (valid for the scattering geometry of our experiments) for the following spin orientations: [100], [010], [001], [110], [101], [011], and [112]. The three $\langle 100 \rangle$ directions correspond to the three possible domain orientations with [100] spin alignment. Similarly for the $\langle 110 \rangle$ directions. However, because the [112] direction leads to such ill-defined polarization behavior we have not included all the equivalent directions. The experimental results should be compared with a single column for a single-domain sample, or with an average over the crystallographically equivalent spin orientations for a sample with multiple domains.

The results in Table I indicate that only the $\langle 100 \rangle$ spin orientations are compatible with our polarization results. Though it may not seem reasonable to extract spin orientation information from such an indirect analysis, one should consider that extracting spin orientations from neutron scat-

tering is also fraught with difficulties: viz, while the identification of the [111] AF propagation direction results directly from the appearance of ‘‘forbidden’’ peaks, spin orientation within these (111) planes requires careful intensity measurements. Domain structure makes this procedure a delicate one. We return to this issue in the next section.

DISCUSSION

NiO, although it is often referred to as ‘‘the classical easy-plane AF,’’ has over the past few years shown that it is very far from being well understood. In this section we will review the issues and, if appropriate, indicate how the present results relate to them.

(i) Two independent Raman observations^{8,9} of the AF magnon have reported that at low temperatures it is a doublet rather than the expected singlet at zero field. The present results confirm this observation. In Ref. 8 it was suggested that the extra peak might be a surface magnon, but this assignment was questioned in Ref. 9 in which the experiments were done in a transmission scattering geometry. A possible explanation is that the doublet corresponds to the two modes expected for an easy-plane AF with in-plane anisotropy.^{10,12} This assignment, however, would require substantially different values of the anisotropy parameters.

(ii) A Brillouin scattering study⁹ showed that there is a low-frequency central peak whose origin is still unknown. This central peak is related to the magnetic properties since it vanishes at the Néel temperature. In that reference it was suggested that the central peak could be the lower branch of the magnon dispersion curve but that its polarization features were not consistent with the expected antisymmetric magnetic scattering. In light of the symmetric nature of scattering from the 38- cm^{-1} mode observed here, this interpretation should perhaps be reconsidered. Such an assignment would require yet another set of anisotropy parameters.

(iii) The same Brillouin scattering investigation produced elastic constant data inconsistent with ultrasonic results. However, above the Néel temperature the Brillouin and ultrasonic results are in better agreement. This is a strong indication that the elastic and magnetic properties of NiO are strongly coupled and that a simultaneous solution to the acoustic phonon-magnon problem may be required. Another indication of possible phonon-magnon coupling is the large, compared with that in other antiferromagnets, linewidth of the AF mode even at $T \ll T_N$.

(iv) Another troubling issue with regard to the magnetic structure of NiO is the direction of the spins. Although it is clear that the AF propagation vector is $[111]$, the spin orientation has been elusive. Early studies of this material suggested the spins lie along $[100]$ directions¹ or $[111]$ directions.¹⁸ Subsequent investigations indicated that the spins lie along either $[110]$ or $[11\bar{2}]$ (Ref. 2) directions. The most recent and generally accepted orientation is along $[11\bar{2}]$.^{5,19} This direction is surprising because it is not possible to obtain an energy extremum along $[11\bar{2}]$. With the usual anisotropy energy of a cubic system²⁰

$$U = A_1(\alpha_1^2\alpha_2^2\alpha_3^2 + \alpha_3^2\alpha_1^2) + A_2(\alpha_1^2\alpha_2^2\alpha_3^2), \quad (4)$$

where A_1 and A_2 are anisotropy constants and the α_i are direction cosines, it is easy to show that the $[11\bar{2}]$ direction cannot have an energy that is simultaneously lower than those of the $[100]$, $[110]$, and $[111]$ directions. Therefore, to account for the $[11\bar{2}]$ orientation it is necessary to either include higher-order anisotropies or to invoke a small deviation from cubic symmetry: Both explanations would emphasize the rather subtle nature of magnetism in this “classical AF.”

(v) The final issue is the strength of the linear magneto-optic coupling terms, specifically the case of NiO and MnF₂. Although we presented arguments as to why linear scattering is small in NiO [i.e., the small prefactor R in Eq. (2)], MnF₂ has a similar prefactor but shows a clear linear coupling term. One possible explanation is simply the magnitude of the K_+ magneto-optic coupling constant in the two materials, in which case a relatively small K_+ for NiO is implied by the experimental results. Another possibility is the inequivalence of the two sublattices in MnF₂, which would lead to out-of-phase scattering as described by Eq. (5.18) of Ref. 13. This equation is almost identical to Eq. (2) except that the prefactor is replaced by its reciprocal (for MnF₂ the prefactor $R=0.09$ is replaced by 11 representing an increase

of more than 120 in the relative intensity). In the Appendix we sketch arguments that account for nonzero out-of-phase contributions to scattering in MnF₂. Although intriguing, these arguments must be treated with caution especially in light of the results of Refs. 16 and 17, where experimental scattering intensities could be reproduced by including only in-phase contributions.

CONCLUSION

NiO, although considered to be one of the classical AF materials, possesses a number of intriguing properties that are strongly suggestive that our understanding of this “simple” system is far from complete. Resolution of the issues listed above will require further experimental work on NiO and on other related compounds (MnO, CoO) and also further theoretical treatments of the light scattering cross section and magnon-phonon interactions.

ACKNOWLEDGMENTS

Work at ANL was supported by the U. S. Department of Energy, Basic Energy Sciences-Materials Sciences under Contract No. W-31-109-ENG-38.

APPENDIX

The spins in the MnF₂ structure occupy sites of D_{2h} symmetry. The linear magneto-optic coupling terms in this symmetry [constrained by Onsager’s relationship $X_{\alpha\beta}(M) = X_{\beta\alpha}(-M)$] lead to $K_{xyz} = -K_{yxz} = a$, $K_{zxy} = -K_{xyz} = b$, and $K_{yzx} = -K_{zyx} = c$. Since the two sublattices are related by a 90° rotation ($x \rightarrow y$, $y \rightarrow -x$), the in- and out-of-phase contributions now depend on $b \pm c$, neither of which is zero by symmetry and hence both in- and out-of-phase scattering are allowed.

¹C. G. Shull, W. A. Strauser, and E. O. Wollan, Phys. Rev. **83**, 333 (1951).

²W. L. Roth, Phys. Rev. **110**, 1333 (1958).

³P. A. Fleury and R. Loudon, Phys. Rev. **166**, 514 (1968).

⁴R. E. Dietz, G. I. Parisot, and A. E. Meixner, Phys. Rev. B **4**, 2302 (1971).

⁵M. T. Hutchings and E. J. Samuelsen, Phys. Rev. B **6**, 3447 (1972).

⁶M. J. Massey, N. H. Chen, J. W. Allen, and R. Merlin, Phys. Rev. B **42**, 8776 (1990).

⁷D. J. Lockwood, *Advances in Magneto-Optics II. Proceedings of the 2nd Symposium on Magneto-Optics* [Fiz. Nizk. Temp. **18** (Suppl. 1), 165 (1992)].

⁸D. J. Lockwood, M. G. Cottam, and J. H. Baskey, J. Magn. Magn. Mater. **104-107**, 1053 (1992).

⁹M. Grimsditch, S. Kumar, and R. S. Goldman, J. Magn. Magn. Mater. **129**, 327 (1994).

¹⁰M. G. Cottam and A. Latiff Awang, J. Phys. C **12**, 105 (1979).

¹¹The numerical results of Cottam and Awang (Ref. 10) for the temperature dependence of the single-magnon excitation in NiO

covered the range $0 < T/T_N < 0.9$ but at a field $H = 19$ kOe. The zero-field values plotted in Fig. 2 are obtained from the relation $E(0) = [(E(H))]^2 - 3(g\mu_B H)^2]^{1/2}$. Since $g\mu_B H = 2$ cm⁻¹ the effect of this correction on the values given in the reference is small.

¹²A. Stevens, J. Phys. C **5**, 1859 (1972).

¹³M. G. Cottam and D. J. Lockwood, *Light Scattering in Magnetic Solids* (Wiley & Sons, New York, 1986).

¹⁴M. G. Cottam, J. Phys. C **8**, 1933 (1975).

¹⁵D. J. Lockwood, M. G. Cottam, V. C. Y. So, and R. S. Katiyar, J. Phys. C **17**, 6009 (1984).

¹⁶D. J. Lockwood and M. G. Cottam, Phys. Rev. B **35**, 1973 (1987).

¹⁷M. G. Cottam, V. P. Gnezdilov, H. J. Labbé, and D. J. Lockwood, J. Appl. Phys. **76**, 6883 (1984).

¹⁸Y. Y. Li, Phys. Rev. **100**, 627 (1955).

¹⁹H. Kondoh and T. Takeda, J. Phys. Soc. Jpn. **19**, 2041 (1964).

²⁰C. Kittel, *Introduction to Solid State Physics* (Wiley, New York, 1971).